The hyperpolarization-activated cyclic nucleotide-gated HCN2 channel transports ammonium in the distal nephron

Rolando Carrisoza-Gaytán[1], Claudia Rangel[1], Carolina Salvador[1], Ricardo Saldaña-Meyer[1], Christian Escalona[1], Lisa M. Satlin[2], Wen Liu[2], Beth Zavilowitz[2], Joyce Trujillo[3], Norma A. Bobadilla[3] and Laura I. Escobar[1]

[1]Departamento de Fisiología, Facultad de Medicina, Universidad Nacional Autónoma de México, México DF, México; [2]Department of Pediatrics, Mount Sinai School of Medicine, New York, New York, USA and [3]Unidad de Fisiología Molecular, Instituto de Investigaciones Biomédicas, Universidad Nacional Autónoma de México, Instituto Nacional de Ciencias Médicas y Nutrición, México DF, México

Recent studies have identified Rhesus proteins as important molecules for ammonia transport in acid-secreting intercalated cells in the distal nephron. Here, we provide evidence for an additional molecule that can mediate NH3/NH4 excretion, the subtype 2 of the hyperpolarization-activated cyclic nucleotide-gated channel family (HCN2), in collecting ducts in rat renal cortex and medulla. Chronic metabolic acidosis in rats did not alter HCN2 protein expression but downregulated the relative abundance of HCN2 mRNA. Its cDNA was identical to the homolog from the brain and the protein was post-translationally modified by *N*-type glycosylation. Electrophysiological recordings in *Xenopus* oocytes injected with HCN2 cRNA found that potassium was transported better than ammonium, each of which was transported significantly better than sodium, criteria that are compatible with a role for HCN2 in ammonium transport. In microperfused rat outer medullary collecting duct segments, the initial rate of acidification, upon exposure to a basolateral ammonium chloride pulse, was higher in intercalated than in principal cells. A specific inhibitor of HCN2 (ZD7288) decreased acidification only in intercalated cells from control rats. In rats with chronic metabolic acidosis, the rate of acidification doubled in both intercalated and principal cells; however, ZD7288 had no significant inhibitory effect. Thus, HCN2 is a basolateral ammonium transport pathway of intercalated cells and may contribute to the renal regulation of body pH under basal conditions.

Kidney International (2011) **80,** 832–840; doi:10.1038/ki.2011.230; published online 27 July 2011

KEYWORDS: acid-base homeostasis; ammonium; collecting duct; hyperpolarization-activated cyclic nucleotide-gated channel; intercalated cell

Correspondence: *Laura I. Escobar, Departamento de Fisiología, Facultad de Medicina, Universidad Nacional Autónoma de México, México DF, México 04510. E-mail: laurae@servidor.unam.mx*

Received 2 August 2010; revised 27 April 2011; accepted 24 May 2011; published online 27 July 2011

The family of hyperpolarization-activated cyclic nucleotide-gated cationic non-selective (HCN) channels has been widely characterized in excitable tissues, where it regulates pacemaker activity.[1–4] Transcripts of HCN isoforms have been found in non-excitable tissues including the liver[3,4] and kidney,[5,6] whereas protein expression of the four HCN isoforms (HCN1–HCN4) has been detected in ovary[7] and pancreatic cells,[8,9] and only HCN2 has been detected in the renal inner medulla.[5] Although it has been accepted that the HCN3 channel has a fundamental role in coordinating peristalsis of the upper urinary tract,[10] the physiological role of HCN channels in non-excitable cells is still uncertain.

Maintenance of salt, water, and acid–base homeostasis is accomplished in the kidney. The proximal tubule reabsorbs 80% of the bicarbonate (HCO_3^-) and 60% of the Na^+ filtered at the glomerulus. Most of the transcellular $NaHCO_3$ reabsorption in the proximal tubule is mediated by the apical Na^+/H^+ exchanger NHE3, which at the same time contributes to most of the NaCl reabsorption.[11] The regulation of plasma HCO_3^- concentration and systemic arterial pH depends critically on the ability of the kidney to produce and secrete ammonium (NH_4^+).[12] The proximal tubule is the principal site of renal NH_4^+ production,[13] as well as an important site of NH_4^+ secretion.[14] Approximately 25% of the filtered Na^+, K^+, Cl^-, and HCO_3^- (ref. 15) and 40–80% of NH_4^+ (ref. 16) delivered out of the proximal tubule are reabsorbed in the thick ascending limb of the loop of Henle and concentrated in the interstitium. Finally, the distal nephron reabsorbs about 5% of the filtered $NaHCO_3^-$ and also excretes NH_4^+ into the urine to maintain the total body acid–base homeostasis. Within the distal nephron, Na^+ absorption is mediated by principal cells, whereas the acid-secreting intercalated cells regulate acid–base homeostasis by contributing to NH_4^+ excretion.[17,18] The acid-secreting intercalated cells secrete H^+ via the luminal vacuolar-type H–ATPase[19] and the H–K–ATPase.[20]

The Rhesus glycoproteins Rhbg and Rhcg were the first ammonia (NH_3) transporters reported in mammals.[21]

However, Rh glycoproteins operate as gas channels and thus transport NH_3 but not NH_4^+.[22,23] Rhbg and Rhcg are found in principal cells and in acid-secreting intercalated cells in distal segments of the nephron.[24] Mice with Rhbg deletion display normal acid–base parameters and basal NH_3 excretion.[25] In contrast, in mice with genetic ablation of Rhcg, urinary NH_4^+ excretion is reduced by 40%.[26] Furthermore, chronic metabolic acidosis (CMA) upregulates Rhcg expression in intercalated cells in the medulla but not in the cortex.[27]

In this work, we identified an immunodetectable HCN2 channel in the rat renal cortex and medulla. To unravel the physiological role of HCN2, we applied different experimental strategies. We examined the effect of CMA on channel expression, isolated complementary DNA and conducted functional studies of HCN2 heterologously expressed in *Xenopus* oocytes, and examined basolateral NH_4^+ uptake (using a fluorescent pH indicator dye) in individually identified cells, in microperfused outer medullary collecting ducts (OMCDs) isolated from control and acidotic animals, in the absence and presence of a specific HCN channel blocker.

RESULTS

HCN2 in the rat kidney

HCN2 was detected by immunoblotting in the rat renal cortex and medulla. Antibodies against HCN2 produced immunoreactive bands corresponding to immature (90 kDa) and *N*-glycosylated (120 kDa) proteins (Figure 1a) as expected, based on previous studies conducted on the brain.[6,28–30] We performed a glycosidase assay to confirm that HCN2 is also glycosylated in the kidney (Figure 1b). HCN2 expression was higher in plasma compared with microsomal membranes isolated from both the cortex and medulla (Figure 1c).

Immunofluorescence analysis also confirmed the presence of HCN2 in the cortex and medulla of rat kidney (Figure 2). To determine the segment and cell type to which the anti-HCN2 antibody bound, double-immunofluorescence assays were performed. Aquaporin 1 antibody was used as a specific marker for proximal tubules. Expression of aquaporin 2 was observed in connecting tubule, cortical collecting duct, OMCD, and inner medullary collecting duct cells (Figure 3, red).[31] HCN2-positive immunoreactivity was detected in connecting tubule and along the collecting ducts. Therefore, we proceeded to stain with antibodies against the H–ATPase B1-subunit, a specific marker of acid-secreting intercalated cells.[17] We found that HCN2 localized to the basolateral membranes of both acid-secreting intercalated and principal cells in the cortex and medulla (Figure 4).

Renal HCN2 complementary DNA

Kidney HCN2 was compared with its homolog the *HCN2* gene in the brain. A conventional PCR strategy was followed to obtain and amplify kidney HCN2. We partially sequenced the NH_2 terminus from glutamate E165 to the proximal S6

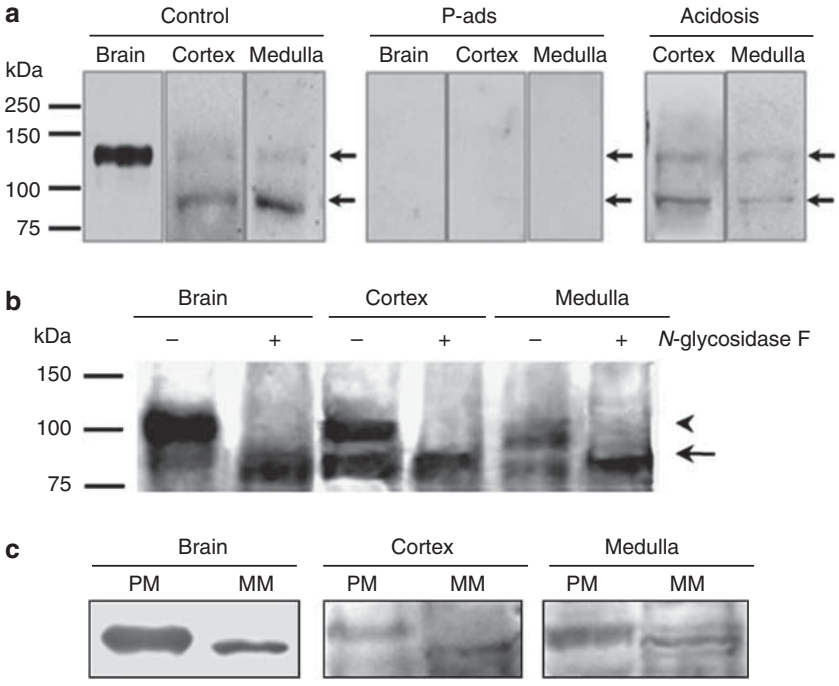

Figure 1 | Subtype 2 of hyperpolarization-activated cyclic nucleotide-gated cationic non-selective (HCN2) protein expression. (**a**) Immunoblotting detection of HCN2 protein in plasma membrane fractions from whole-rat brain, renal cortex, and medulla from control rats (left) and from rats subjected to 5 days of dietary acid loading (right). No immunoreactivity was detected after adsorption of HCN2 antibodies with their corresponding antigens (P-ads). (**b**) HCN2 antibody identified ~120 kDa (glycosylated) and ~90 kDa (unglycosylated) bands (arrowhead and arrow, respectively) in control samples. Only the 90 kDa band was detected when samples (100 μg) were incubated with glycosidase (5 U). (**c**) HCN2 immunoblotting was performed with 100 μg of plasma membranes (PMs) and microsomes (MMs). P-ads, peptide adsorption.

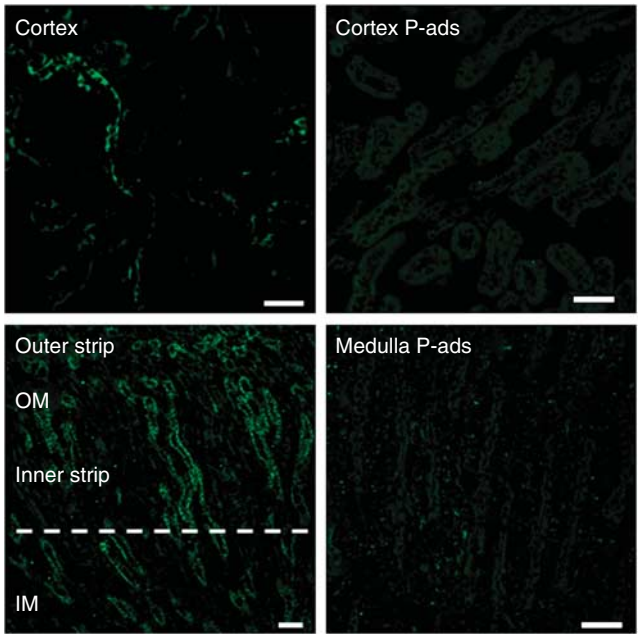

Figure 2 | Immunofluorescence detection of subtype 2 of hyperpolarization-activated cyclic nucleotide-gated cationic non-selective (HCN2) channels. Sagittal sections display positive immunoreactivity for HCN2 in the cortex and in the outer (OM) and inner medulla (IM). Suppression of immunoreactivity is shown when antibodies are preincubated with an excess of control peptide (P-ads) 1 h before the overnight incubation. Bar = 50 μm.

segment, corresponding to 50% of the CNBD-binding domain, up to phenylalanine F580. This amplified kidney HCN2 ccomplementary DNA encodes a protein of 415 amino acids with a 100% identity to brain HCN2 (not shown).

Effect of metabolic acidosis on HCN2 expression

Consumption of an acid load leads to an adaptive increase in renal acid excretion that demands activation and/or regulation of various acid–base transport pathways. These include increased ammoniagenesis, excretion of titratable acids, generation of HCO_3^-, and H^+ secretion. Adaptation is also associated with changes in electrolyte and water handling and with extensive remodeling of the nephron.[14–17] In this context, we examined the effect of chronic NH_4Cl intake (that is, acid loading) on the expression of HCN2. As shown in Table 1, CMA led to an increase in blood urea nitrogen and serum chloride concentration and in a significant fall in serum HCO_3^- concentration as expected.[32] CMA was also associated with a significant reduction ($\sim$60%, $P<0.0006$) in the relative mRNA abundance of HCN2 in the cortex; in contrast, no changes were detected in the medulla (Figure 5b). However, CMA did not elicit changes in HCN2 protein expression in total membranes from the cortex (Supplementary Figure S1 online), neither in microsomes nor in plasma membranes from the cortex and medulla (Figure 5c). Immunolabeling studies of kidneys harvested from animals subjected to CMA did not show changes in the cellular distribution of HCN2 in collecting ducts but revealed diffuse labeling along the thin descending limbs in the medulla (Supplementary Figure S2 online).

HCN2 channels transport NH_4^+ ions

Acid-secreting intercalated cells participate in the renal regulation of acid–base homeostasis and constitute the exclusive site where transepithelial transport allows for NH_4^+ excretion into the urine.[17] As HCN2 was localized to the basolateral membrane (Figure 4), suggesting a role in transepithelial transport, we sought to conduct functional studies of HCN2 expressed in *Xenopus laevis* oocytes. We measured the ionic currents of the heterologously expressed channel and found that HCN2 transported $K^+ > NH_4^+ >> Na^+$ (Figure 6a). The following relative current ionic ratios were estimated: $K/NH_4 = 1.95 \pm 0.096$, $K/Na = 7.28 \pm 0.54$, and $NH_4/Na = 3.75 \pm 0.37$ (Figure 6b). The amplitude of NH_4^+ currents increased with NH_4Cl concentration, and their inhibition by ZD7298, a specific HCN channel blocker,[33] depended on the external $[NH_4^+]$ (Supplementary Figure S3 online). Also, Ba^{2+} inhibited NH_4^+ currents (Supplementary Figure S4 online), a result similar to that reported previously for native and cloned hyperpolarization-activated HCN channels.[34]

NH_4^+ uptake by HCN2 in isolated tubules from OMCD

To test whether HCN2 also conducts NH_4^+ in the native OMCD, we applied the NH_4Cl pulse technique to microperfused control rat OMCDs loaded with 15 μM of the acetoxymethyl ester of 2′7′-bis(-2-carboxyethyl)-5(and 6)-carboxyfluorescein (BCECF) (Invitrogen, Carlsbad, CA) to examine the sensitivity of basolateral NH_4^+ uptake to ZD7298. The initial slope of acidification (the 490/440 nm fluorescence intensity ratio/1000 s) in acid-secreting intercalated cells in ZD7288-treated OMCDs exposed to bath NH_4Cl (1.47 ± 0.49; $n = 6$) was significantly less than that observed in untreated cells (2.89 ± 0.47; $n = 6$; $P < 0.05$; Figure 7). The inhibitor was without effect on the slope of acidification measured in principal cells in the same tubules (Figure 7). OMCDs isolated from acid-loaded rats showed a twofold higher rate of acidification in acid-secreting intercalated cells and in principal cells. However, the rate of acidification was not affected by 10 μM ZD7298 in either cell type in tubules isolated from CMA rats.

DISCUSSION

Our data show that HCN2 is localized to cells in the distal nephron of the cortex and medulla. HCN channels are cation selective but only weakly selective for K^+ over Na^+, with variable permeability ratios of about 5:1 (refs 4,35,36). Because NH_4^+ and K^+ have an identical hydrodynamic radius,[37] it is not surprising that NH_4^+ permeates HCN channels. In fact, NH_4^+ can produce HCN pacemaker currents in photoreceptors.[38] Despite the HCN channel preference for conducting K^+, under physiological conditions, native inward currents will be carried predominantly by Na^+ because of its greater electrochemical gradient. However, metabolic conditions are expected to influence the

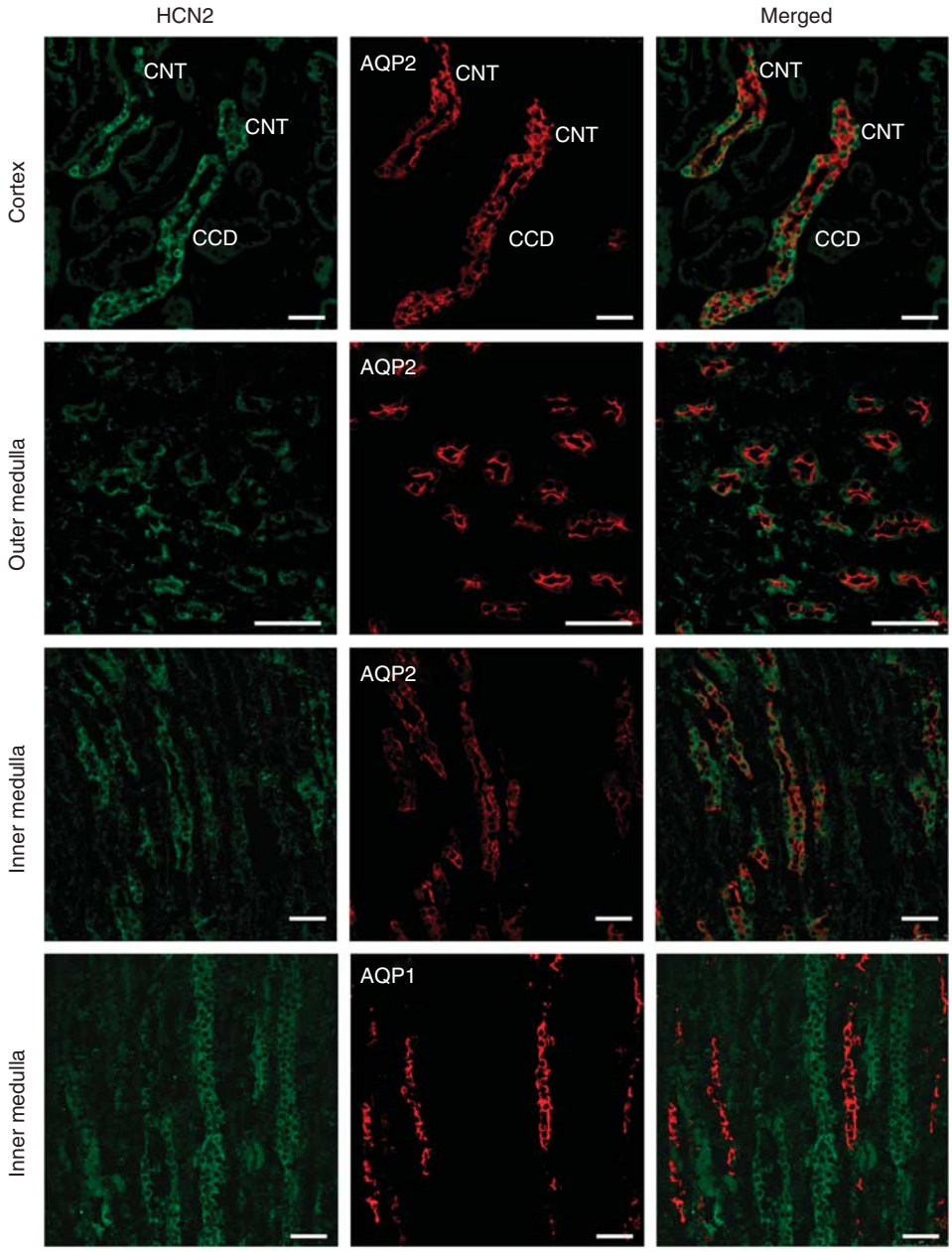

Figure 3 | Subtype 2 of hyperpolarization-activated cyclic nucleotide-gated cationic non-selective (HCN2) channels is localized to distal nephron segments in the rat cortex and in the outer and inner medulla. Sections were colabeled with antibodies directed against HCN2 and aquaporin 2 (AQP2) or aquaporin 1 (AQP1), visualized with secondary antibodies conjugated to Alexa 488 (green) and Alexa 594 (red (Invitrogen, Carlsbad, CA)). HCN2 is expressed exclusively in the connecting and collecting ducts (merged). Bar = 50 μm. CCD, cortical collecting duct; CNT, connecting tubule.

cation selectivity of HCN2 channels in the distal nephron in order to maintain electrolyte and acid–base homeostasis.

The renal response to metabolic acidosis includes increased expression of various ion transport proteins that contribute to increased synthesis and excretion of NH_4^+ and the net production and absorption of HCO_3^-. This adaptation allows the kidney to enhance ammoniagenesis and gluconeogenesis from plasma glutamine to recover acid–base balance. NH_4^+ accumulates in the renal medulla during acidosis, provoking countercurrent multiplication and energy-dependent recycling between the ascending (tALH) and descending thin limbs (tDLH)[39] and the thick ascending limb of Henle's loop.[17] Approximately 80% of NH_4^+ excreted in the urine is translocated across the acid-secreting intercalated cells of the collecting duct.[40]

HCN2 protein expression was not regulated by CMA in plasma membranes from the cortex and medulla, and therefore HCN2 appears to be a constitutive membrane protein in the distal nephron. In contrast, in CMA, protein upregulation of HCN2 in tDLH (Supplementary Figure S2 online) suggests that HCN2 serves as an NH_4^+ entry pathway that

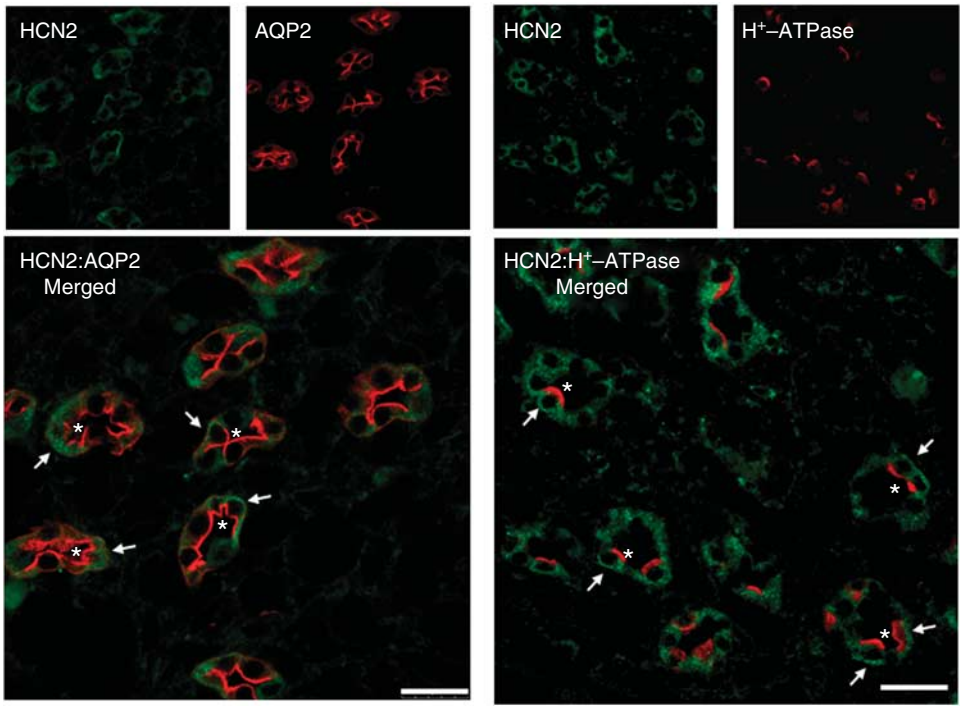

Figure 4 | Immunolocalization of subtype 2 of hyperpolarization-activated cyclic nucleotide-gated cationic non-selective (HCN2) channels in principal and acid-secreting cells in the outer medullary collecting duct. Double-immunofluorescence labeling with antibodies directed against HCN2 (secondary: Alexa 488; green) and aquaporin 2 (AQP2; secondary: Alexa 594; red) or the H–ATPase B1-subunit (secondary: Alexa 594; red). Cells that express both HCN2 and AQP2 or H–ATPase are shown in the bottom panels (merged). AQP2 and H–ATPase are observed in apical membranes (*), whereas HCN2 is in the basolateral membranes (arrows). Bar = 25 μm.

Table 1 | Blood composition and urine pH from control and acidotic rats

Group	BW (g)	pH urine	Cl^- (meq/l)	Na^+ (meq/l)	K^+ (meq/l)	CO_2 (meq/l)	BUN (meq/dl)	SCr (mg/dl)
Control, *n*=7	215 ± 0.8	6.7 ± 0.07	122 ± 4.7	149 ± 1.3	3.8 ± 0.3	19.2 ± 1.6	22.9 ± 1.5	0.48 ± 0.1
Acidosis (5 days), *n*=5	209 ± 6	5.9 ± 0.01	136 ± 2	149 ± 1.1	2.8 ± 0.3	11.2 ± 0.8	31.8 ± 3.4	0.36 ± 0.04
P-value	NS	0.000003	0.03	NS	NS	0.002	0.02	0.02

Abbreviations: BUN, blood urea nitrogen; BW, body weight; Cr, creatinine; NS, not significant; SCr, serum Cr.
Serum electrolytes, total CO_2, Cr, and BUN levels were measured in control rats (water; *n*=7) or in those subjected to metabolic acidosis (280 mM NH_4Cl intake for 5 days; *n*=5). Values are means ± s.e.

facilitates the passive secretion of NH_4^+ and then the counter-current multiplication of NH_4^+ in the rat renal medulla.

Control experiments in oocytes show that block by ZD7288 decreases when $[NH_4^+]_o$ is elevated (Supplementary Figure S3 online), as suggested by Cheng *et al.*[41] ZD7288-induced block of HCN2 is voltage dependent and modulated by $[K^+]_o$. This voltage-dependent block seems to be caused by an increased influx of permeant ions (K^+, NH_4^+, and Na^+) that relieves channel block, similar to the $[K^+]_o$-dependent clearing of tetraethylammonium from the inner pore of delayed rectifier K^+ channels in squid axon.[42]

We detected a strong expression of immunodetectable HCN2 channel in both acid-secreting intercalated cells and principal cells. However, the activity of the channel, measured as inhibitor-specific intracellular acidification following exposure to basolateral NH_4Cl, was detected only in acid-secreting intercalated cells under basal conditions (control, Figure 7b). Our inability to detect robust HCN2 activity in principal cells does not support the hypothesis that HCN2 participates in pH homeostasis. What can be the function of HCN2 channels in principal cells then? Our findings predict that Na^+ can enter principal cells by HCN2 and favor K^+ secretion by potassium channels. In fact, urinary K^+ secretion in the cortical collecting duct depends on both apical and basolateral Na^+ entry.[43] Na^+ entry via HCN2 channels in principal cells might be an alternative pathway for providing substrate for and stimulating Na^+–K^+–ATPase activity in the absence of luminal Na^+ entry, as has also been proposed for the basolateral Na^+/H^+ exchanger.[43] Furthermore, Na^+ might also enter acid-secreting intercalated cells by HCN2 channels and favor K^+ secretion by Kv1.3 channels in animals fed a high K^+ diet, as we described recently.[44] In conclusion, the function of cation-non-selective HCN2 channels in responding to variations in renal metabolism

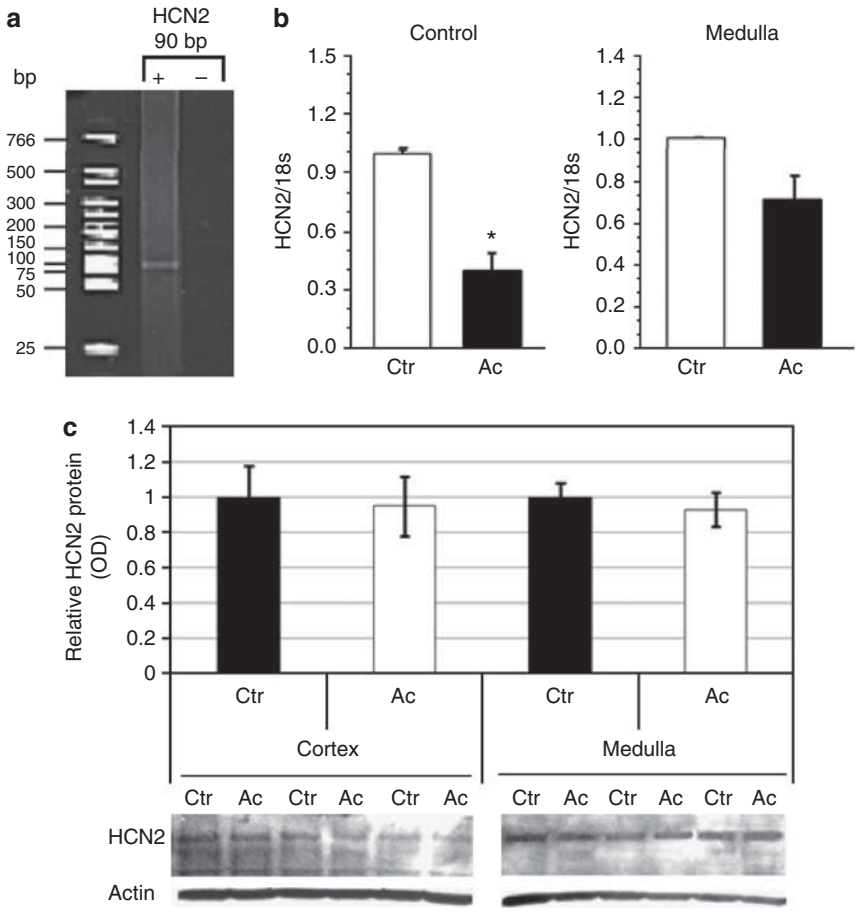

Figure 5 | Effect of chronic acidosis on subtype 2 of hyperpolarization-activated cyclic nucleotide-gated cationic non-selective (HCN2) expression. (**a**) Polyacrylamide gel showing HCN2 amplification from renal cortex total RNA in the presence (+) or absence (−) of reverse transcriptase by using real-time PCR probes after 32 cycles of amplification. The reverse transcription-PCR yielded the expected size product of 90 bp for HCN2. No genomic DNA amplification was observed. (**b**) The relative mRNA expression of HCN2 in control (white bars) and acid-loaded (black bars) rats is shown in the cortex and medulla ($n = 5$). *$P < 0.05$ versus the control group. (**c**) Representative immunoblots of HCN2 in plasma membranes from the renal cortex and medulla of rats adapted to chronic acidosis. No changes in HCN2 expression were observed. Protein (100 μg) was loaded on each lane. Values are mean ± s.e.; $n = 10$ in each dietary group. Ac, acidosis; Ctr, control; OD, optical density.

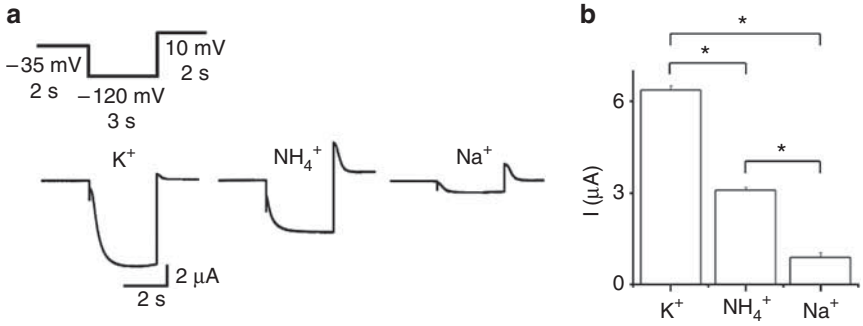

Figure 6 | Subtype 2 of hyperpolarization-activated cyclic nucleotide-gated cationic non-selective (HCN2) channels transport ammonium (NH_4^+). (**a**) Currents were activated from a holding potential of −35 mV for 2 s; voltage was clamped at −120 mV for 3 s, followed by a +10 mV step for 2 s.[41] (**b**) Results are presented as mean ± s.e. Statistical analysis was performed using Student's two-sample paired *t*-tests. Differences were considered significant at $P < 0.01$ (*); $n = 4$.

is likely determined by the repertoire of ion transporters expressed in principal cells and in acid-secreting intercalated cells.

HCN channels are half-maximally activated ($V0.5$) in the voltage range from –60 to –100 mV;[45] however, $V0.5$ can be displaced toward depolarizing values depending on the cell

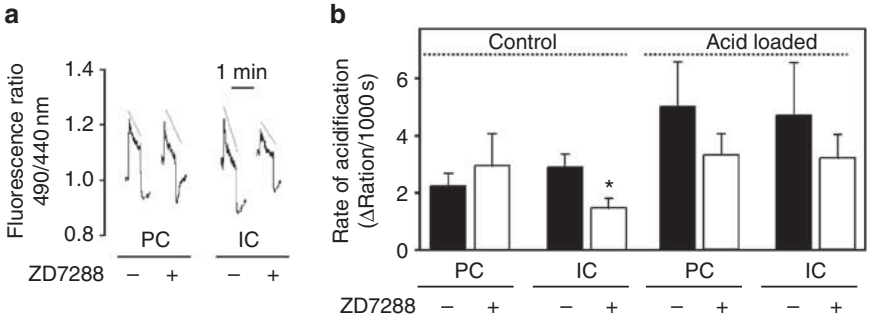

Figure 7 | (Ammonium) NH_4^+ uptake by subtype 2 of hyperpolarization-activated cyclic nucleotide-gated cationic non-selective (HCN2) channels in microperfused rat outer medullary collecting ducts (OMCDs). (**a**) Effect of the HCN2 inhibitor ZD7288 (10 μM) on the response of OMCD principal (PC) and acid-secreting intercalated (IC) cells to an NH_4Cl pulse. OMCDs were loaded with 15 μM of the acetoxymethyl ester of 2′7′-bis(-2-carboxyethyl)-5(and 6)-carboxyfluorescein (BCECF) (Supplementary Material online). The fluorescence ratio intensities (FIRs; 490/440 nm) were measured over time in individually identified cells in untreated and inhibitor-treated OMCDs. The mechanisms accounting for the three phases of the response (initial alkalinization, slow acidification, and then rapid acidification) are discussed in Supplementary Material online. The slopes of the slow acidification (measured over the initial 60 s and normalized to 1000 s) were calculated by exponential curve fitting of the fall in FIR from the peak value. (**b**) Sensitivity of basolateral NH_4^+ uptake into OMCD intercalated and principal cells to 10 μM ZD7288, an inhibitor of HCN2. In microperfused control rat OMCDs, ZD7288 led to a statistically significant reduction in the slope of acidification (over the first minute; presumably reflecting NH_4^+ entry across the basolateral membrane; $^*P<0.05$) in acid-secreting intercalated but not principal cells. In OMCDs isolated from rats adapted to chronic acidosis, ZD7288 did not produce a significant effect.

environment. Acid-secreting intercalated cells in the rat connecting tubule and cortical collecting duct are characterized by a low membrane potential (–36 mV).[46] Therefore, HCN2 channels to be activated must be modulated by extra- and/or intracellular factors. In fact, HCN2 voltage activation is profoundly shifted to more positive potentials by cyclic AMP,[45] endogenous phosphatidylinositol 4,5-biphosphate,[47,48] and by activation of P38 mitogen-activated protein kinase.[49] In addition, bicarbonate has also a stimulatory effect on the generation of cyclic AMP by a soluble adenylyl cyclase in acid-secreting intercalated cells.[50] Furthermore, currents carried by HCN2 show strong Cl^- dependence.[51]

Our inability to detect a significant effect of ZD7288 on the acidification rate in acid-secreting intercalated cells in OMCDs isolated from acidotic rats was unexpected. Similar to native HCN, HCN2 is modulated by cytosolic pH and is not sensitive to changes in external pH. Intracellular acidification induces a downregulation of the current by shifting the activation curve to the left and also slows down the speed of activation. In contrast, alkalinization enhances the current by shifting the activation curve to more depolarized voltages and, in addition, accelerates opening kinetics.[52] As the resting pHi in acid-secreting intercalated cells (namely, ~7.2) is unaltered during CMA, presumably because of adaptation of the efficient H^+ extrusion pathways and intracellular buffering,[53] one cannot attribute the loss of inhibitor sensitivity to a CMA-induced change in pHi. Clearly, further studies will be necessary to unravel the role of HCN2 in CMA.

OMCDs isolated from acid-loaded rats showed a twofold higher rate of acidification in acid-secreting intercalated cells and in principal cells than was detected under control conditions. These results suggest that the increased rate of acidification in microperfused tubules from animals subjected to CMA may be due to enhanced apical and/or basolateral expression of other NH_3 transport pathways, including the NH_3 transporter family member Rhcg in principal cells and in acid-secreting intercalated cells.[54]

Although one may argue that the most precise evidence supporting a physiological role of HCN2 in the renal regulation of acid–base homeostasis would be to study mice with targeted deletion of HCN2 in acid-secreting intercalated cells, adaptation of the animals to the loss of the gene product by upregulation of alternate pathways for NH_4^+ excretion may impact expression of a phenotype. Therefore, future studies should be directed to generating conditional knockouts of HCN2 in the unique cell populations comprising the collecting duct.

There has been extensive investigation focused on identifying the specific transport proteins in acid-secreting intercalated cells responsible for basolateral NH_4^+ uptake, a necessary step in urinary acidification. The Na/K/2Cl cotransporter NKCC1 is expressed in the basolateral membrane of acid-secreting intercalated cells in the OMCD and inner medullary collecting duct.[55] However, NKCC1 does not seem to participate in NH_4^+ transport in acid-secreting intercalated cells.[56] NH_4^+ uptake by Na–K–ATPase is an important determinant of pHi and net acid secretion but only in the rat terminal inner medullary collecting duct.[57]

Importantly, Rhcg found in principal cells and in acid-secreting intercalated cells appears to account partially for basal NH_3 excretion and to contribute to increased NH_3 excretion with CMA.[26,58]

In summary, our findings demonstrate that basolateral HCN2 is a pathway for NH_4^+ uptake in acid-secreting intercalated cells under basal conditions, suggesting its participation in NH_4^+ transepithelial transport and, in turn, in urinary NH_4^+ excretion in the distal nephron of the

mammalian kidney. Future experiments must be performed to elucidate the role of HCN2 in CMA in the distal nephron.

MATERIALS AND METHODS

Care and handling of animals

See Supplementary Material online.

RNA purification and reverse transcription-PCR

Total RNA was isolated as described by Carrisoza-Gaytán.[44] Complementary DNA was synthesized from 5 μg of cortex RNA using the random primer p(dN)6 (Roche Diagnostics, Rotkreuz, Switzerland) and reverse transcribed with MLV reverse trancriptase (Invitrogen) according to the manufacturer's instructions. A set of primers were designed, derived from the exon sequences of rat HCN2 (NM_053684). Exons 2–4 were amplified with degenerate primers 5′-TGCTG CAGCCKGGSGTCAACAARTTCTCCCT-3′ (sense) and 5′-CATGTAC TGCTCCACYTGCTTGTACTTCTC-3′ (antisense); exons 5 and 6 were amplified with primers 5′-TACAAGCAAGTGGAGCAG-3′ (sense) and 5′-CCCCAAAATAGGAGCCAT-3′ (antisense). DNA fragments were amplified, purified, and sequenced as reported by Carrisoza-Gaytán.[44]

Real-time reverse transcription-PCR

Reverse transcription was carried out with 2.5 μg of total RNA using 200 U of Moloney murine leukemia virus reverse transcriptase (Invitrogen). The mRNA levels of HCN2 were quantified using the ABI Prism 7300 Sequence Detection System (*Taq*Man, Applied Biosystems, ABI, Foster City, CA). Primers and probes were ordered as Rn01408575_gH (Assays-on-Demand, ABI). As an endogenous control, we used eukaryotic 18S rRNA (predesigned assay reagent applied by ABI, external run). The relative quantification of gene expression was performed using the comparative Connecticut method.[59]

Western blot analysis

Membrane sample extraction was performed as previously described.[44,60] Plasma membranes were obtained by centrifugation at 17,000 *g* for 20 min and microsomes at 150,000 *g* for 1 h at 4 °C. Immunoblots were performed with a rabbit anti-HCN2 antibody from Alomone (Jerusalem, Israel) (1:200) following procedures previously established.[44,60] Membrane samples (100 μg) were electrophoretically separated in 10% SDS-polyacrylamide gel electrophoresis and electroblotted to a nylon membrane. Non-fat dry milk (5%) (Bio-Rad, Hercules, CA) in TBS-T (20 mM Tris-HCl, 136 mM NaCl, 0.1% Tween 20, pH 7.6) was added for 1 h. Each blot was first incubated with an anti-HCN2 antibody at 4 °C overnight and then with donkey anti-rabbit IgG coupled to horseradish peroxidase (1:5000; Amersham Biosciences, Freiburg, Germany), the secondary antibody, for 1 h. Immunoblots were detected using ECL plus detection reagents (Amersham Biosciences).

Glycosidase assay

The procedure is described in Supplementary Material online.

Immunofluorescence assays

Procedures are described in detail in Supplementary Material online.

HCN2 expression and electrophysiological assays in *Xenopus laevis* oocytes

Procedures are described in Supplementary Material online.[61]

NH_4^+ uptake assay in microperfused rat OMCD

The methodology is described in detail in Supplementary Material online.[62–66]

DISCLOSURE

All the authors declared no competing interests.

ACKNOWLEDGMENTS

We thank Michael Sanguinetti and Steven Siegelbaum for the mouse brain HCN2 cDNA and Maria Jose Gomora for assistance with the confocal microscope (Grant SDI-PTID.05.01) and the PhD program (Ciencias Biomédicas, UNAM). This work was supported by DGAPA Grants IN224406 and IN202110-3 (LIE) at the UNAM; by Conacyt Grant 48483 (NAB); by scholarships from Conacyt (RCG, CR, RSM, and JT); and by National Institutes of Health Grants DK051391 and P30 DK079307 (The Pittsburgh Center for Kidney Research; LMS).

SUPPLEMENTARY MATERIAL

Figure S1. Effect of chronic metabolic acidosis on subtype 2 of hyperpolarization-activated cyclic nucleotide-gated cationic non-selective (HCN2) channel expression.

Figure S2. Immunolocalization of subtype 2 of hyperpolarization-activated cyclic nucleotide-gated cationic non-selective (HCN2) channel in the inner medullary collecting duct and papilla from rats adapted to CMA.

Figure S3. HCN2 current traces as a function of NH_4Cl concentrations and inhibition of the whole-cell hyperpolarization activated current by ZD7288.

Figure S4. Block of the whole-cell hyperpolarization activated I_{HCN2} current by Ba^{2+}.

Supplementary material is linked to the online version of the paper at http://www.nature.com/ki

REFERENCES

1. DiFrancesco D. Pacemaker mechanisms in cardiac tissue. *Annu Rev Physiol* 1993; **55**: 455–472.
2. Luthi A, McCormick DA. H-current: properties of a neuronal and network pacemaker. *Neuron* 1998; **21**: 9–12.
3. Santoro B, Liu DT, Yao H *et al.* Identification of a gene encoding a hyperpolarization-activated pacemaker channel of brain. *Cell* 1998; **93**: 717–729.
4. Santoro B, Tibbs GR. The HCN gene family: molecular basis of the hyperpolarization-activated pacemaker channels. *Ann N Y Acad Sci* 1999; **868**: 741–764.
5. Bolivar JJ, Tapia D, Arenas G *et al.* A hyperpolarization-activated, cyclic nucleotide-gated, (Ih-like) cationic current and HCN genes expression in renal inner medullary collecting duct cells. *Am J Physiol Cell Physiol* 2008; **294**: C893–C906.
6. Uawithya P, Pisitkun T, Ruttenberg BE *et al.* Transcriptional profiling of native inner medullary collecting duct cells from rat kidney. *Physiol Genomics* 2008; **32**: 229–253.
7. Yeh J, Kim BS, Gaines L *et al.* The expression of hyperpolarization activated cyclic nucleotide gated (HCN) channels in the rat ovary are dependent on the type of cell and the reproductive age of the animal: a laboratory investigation. *Reprod Biol Endocrinol* 2008; **6**: 35.
8. El-Kholy W, MacDonald PE, Fox JM *et al.* Hyperpolarization-activated cyclic nucleotide-gated channels in pancreatic beta-cells. *Mol Endocrinol* 2007; **21**: 753–764.
9. Zhang Y, Zhang N, Gyulkhandanyan AV *et al.* Presence of functional hyperpolarization-activated cyclic nucleotide-gated channels in clonal alpha cell lines and rat islet alpha cells. *Diabetologia* 2008; **51**: 2290–2298.
10. Hurtado R, Bub G, Herzlinger D. The pelvis–kidney junction contains HCN3, a hyperpolarization-activated cation channel that triggers ureter peristalsis. *Kidney Int* 2003; **77**: 500–508.
11. Aronson PS, Giebisch G. Mechanism of chloride transport in the proximal tubule. *Am J Physiol Renal Physiol* 1997; **273**: F179–F192.
12. Halperin ML, Goldstein MS, Steinbaugh BJ *et al.* Biochemistry and physiology of ammonium excretion. In: Seldin DW, Giebisch G (eds). *The Kidney: Physiology and Pathophysiology*. Raven Press Company: New York, 1985, pp 1471–1490.
13. Good DW, Burg MB. Ammonia production by individual segments of the rat nephron. *J Clin Invest* 1984; **73**: 602–610.
14. Good DW, DuBose TD. Ammonia transport by early and late proximal convoluted tubule of the rat. *J Clin Invest* 1987; **79**: 684–691.

15. Good DW. Regulation of bicarbonate and ammonium absorption in the thick ascending limb of the rat. *Kidney Int* 1991; **40**: S36–S42.
16. Attmane-Elakeb A, Amlal H, Bichara M. Ammonium carriers in medullary thick ascending limb. *Am J Physiol* 2001; **280**: F1–F9.
17. Hamm LL, Alpern RJ, Preisig PA. Cellular mechanisms of renal tubular acidification. In: Alpern RJ, Hebert SC (eds). *The Kidney: Physiology and Pathophysiology*. Elsevier Company: Amsterdam, 2008, pp 1539–1585.
18. Schuster VL. Bicarbonate reabsorption and secretion in the cortical and outer medullary collecting tubule. *Semin Nephrol* 1990; **10**: 139–147.
19. Brown D, Paunescu TG, Breton S *et al.* Regulation of the V-ATPase in kidney epithelial cells: dual role in acid-base homeostasis and vesicle trafficking. *J Exp Biol* 2009; **212**: 1762–1772.
20. Wingo CS, Smolka AJ. Function and structure of H-K-ATPase in the kidney. *Am J Physiol* 1995; **269**: F1–F16.
21. Marini AM, Matassi G, Raynal V *et al.* The human Rhesus-associated RhAG protein and a kidney homologue promote ammonium transport in yeast. *Nat Genet* 2000; **26**: 341–344.
22. Khademi S, O'Connell III J, Remis J *et al.* Mechanism of ammonia transport by Amt/MEP/Rh: structure of AmtB at 1.35 A. *Science* 2004; **305**: 1587–1594.
23. Zheng L, Kostrewa D, Berneche S *et al.* The crystal structure of AmtB of E. coli suggests a mechanism for ammonia transport. *Proc Natl Acad Sci* 2004; **101**: 17090–17095.
24. Quentin F, Eladari D, Cheval L *et al.* RhBG and RhCG, the putative ammonia transporters, are expressed in the same cells in the distal nephron. *J Am Soc Nephrol* 2003; **14**: 545–554.
25. Chambrey R, Goossens D, Bourgeois S *et al.* Genetic ablation of Rhbg in the mouse does not impair renal ammonium excretion. *Am J Physiol Renal Physiol* 2005; **289**: F1281–F1290.
26. Biver S, Belge H, Bourgeois S *et al.* A role for Rhesus factor Rhcg in renal ammonium excretion and male fertility. *Nature* 2008; **456**: 339–343.
27. Seshadri RM, Klein JD, Kozlowski S *et al.* Changes in subcellular distribution of the ammonia transporter, Rhcg, in response to chronic metabolic acidosis. *Am J Physiol Renal Physiol* 2006; **290**: F1443–F1452.
28. Bakondi G, Pór A, Kovács I *et al.* Hyperpolarization-activated, cyclic nucleotide-gated, cation non-selective channel subunit expression pattern of guinea-pig spiral ganglion cells. *Neuroscience* 2009; **158**: 1469–1477.
29. Brewster AL, Chen Y, Bender RA *et al.* Quantitative analysis and subcellular distribution of mRNA and protein expression of the hyperpolarization-activated cyclic nucleotide-gated channels throughout development in rat hippocampus. *Cereb Cortex* 2007; **17**: 702–712.
30. Mistrík P, Mader R, Michalakis S *et al.* The murine HCN3 gene encodes a hyperpolarization-activated cation channel with slow kinetics and unique response to cyclic nucleotides. *J Biol Chem* 2005; **280**: 27056–27061.
31. Coleman RA, Wu DC, Liu J *et al.* Expression of aquaporins in the renal connecting tubule. *Am J Physiol Renal Physiol* 2000; **279**: F874–F883.
32. Faroqui S, Sheriff S, Amlal H. Metabolic acidosis has dual effects on sodium handling by rat kidney. *Am J Physiol Renal Physiol* 2006; **291**: F322–F331.
33. Zagotta WN, Siegelbaum SA. Structure and function of cyclic nucleotide-gated channels. *Annu Rev Neurosci* 1996; **19**: 235–263.
34. van Welie I, Wadman WJ, van Hooft JA. Low affinity block of native and cloned hyperpolarization-activated Ih channels by Ba^{2+} ions. *Eur J Pharmacol* 2005; **507**: 15–20.
35. Ludwig A, Zong X, Hofmann F *et al.* Structure and function of cardiac pacemaker channels. *Cell Physiol Biochem* 1999; **9**: 179–186.
36. Biel M, Wahl-Schott C, Michalakis S *et al.* Hyperpolarization-activated cation channels: from genes to function. *Physiol Rev* 2009; **89**: 847–885.
37. Atkins PW. Molecules in motion: ion transport and molecular diffusion. In: Atkins PW (ed). *Physical Chemistry*. Oxford University Press: Oxford, 1978, pp 893–897.
38. Wollmuth LP, Hille B. Ionic selectivity of Ih channels of rod photoreceptors in tiger salamanders. *J Gen Physiol* 1992; **100**: 749–765.
39. Flessner MF, Mejia R, Knepper MA. Ammonium and bicarbonate transport in isolated perfused rodent long-loop thin descending limbs. *Am J Physiol* 1993; **264**: F388–F396.
40. Ibrahim H, Lee YJ, Curthoys NP. Renal response to metabolic acidosis: role of mRNA stabilization. *Kidney Int* 2008; **73**: 11–18.
41. Cheng L, Kinard K, Rajamani R *et al.* Molecular mapping of the binding site for a blocker of hyperpolarization-activated, cyclic nucleotide-modulated pacemaker channels. *J Pharmacol Exp Ther* 2007; **322**: 931–939.
42. Armstrong CM. Interaction of tetraethylammonium ion derivatives with the potassium channels of giant axons. *J Gen Physiol* 1971; **58**: 413–437.
43. Muto S, Tsuruoka S, Miyata Y *et al.* Basolateral Na+/H+ exchange maintains potassium secretion during diminished sodium transport in the rabbit cortical collecting duct. *Kidney Int* 2009; **75**: 25–30.
44. Carrisoza-Gaytán R, Salvador C, Satlin LM *et al.* Potassium secretion by the voltage gated potassium channel Kv1.3 in the rat kidney. *Am J Physiol Renal Physiol* 2010; **299**: F255–F264.
45. Robinson RB, Siegelbaum SA. Hyperpolarization-activated cation currents: from molecules to physiological function. *Annu Rev Physiol* 2003; **65**: 453–480.
46. Palmer LG, Frindt G. High conductance K channels in intercalated cells of the rat distal nephron. *Am J Physiol Renal Physiol* 2007; **292**: F966–F973.
47. Zolles G, Klöcker N, Wenzel D *et al.* Pacemaking by HCN channels requires interaction with phosphoinositides. *Neuron* 2006; **52**: 1027–1036.
48. Pian P, Bucchi A, Robinson RB *et al.* Regulation of gating and rundown of HCN hyperpolarization-activated channels by exogenous and endogenous PIP2. *J Gen Physiol* 2006; **128**: 593–604.
49. Poolos NP, Bullis JB, Roth MK. Modulation of h-channels in hippocampal pyramidal neurons by p38mitogen-activated protein kinase. *J Neurosci* 2006; **26**: 7995–8003.
50. Pastor-Soler N, Beaulieu V, Litvin TN *et al.* Bicarbonate-regulated adenylyl cyclase (sAC) is a sensor that regulates pH-dependent V-ATPase recycling. *J Biol Chem* 2003; **278**: 49523–49529.
51. Wahl-Schott C, Baumann L, Zong X *et al.* An arginine residue in the pore region is a key determinant of chloride dependence in cardiac pacemaker channels. *J Biol Chem* 2005; **280**: 13694–13700.
52. Zong X, Stieber J, Ludwig A *et al.* A single histidine residue determines the pH sensitivity of the pacemaker channel HCN2. *J Biol Chem* 2001; **276**: 6313–6319.
53. Silver RB, Mennitt PA, Satlin LM. Stimulation of apical H-K-ATPase in intercalated cells of cortical collecting duct with chronic metabolic acidosis. *Am J Physiol* 1996; **270**: F539–F547.
54. Seshadri RM, Klein JD, Smith T *et al.* Changes in subcellular distribution of the ammonia transporter, Rhcg, in response to chronic metabolic acidosis. *Am J Physiol Renal Physiol* 2006; **290**: F1443–F1452.
55. Ginns SM, Knepper MA, Ecelbarger CA *et al.* Immunolocalization of the secretory isoform of Na-K-Cl cotransporter in rat renal intercalated cells. *J Am Soc Nephrol* 1996; **7**: 2533–2542.
56. Wall SM, Fischer MP. Contribution of the Na(+)-K(+)-2Cl(−) cotransporter (NKCC1) to transepithelial transport of H(+), NH(4)(+), K(+), and Na(+) in rat outer medullary collecting duct. *J Am Soc Nephrol* 2002; **13**: 827–835.
57. Wall SM. Ouabain reduces net acid secretion and increases pHi by inhibiting NH4+ uptake on rat tIMCD Na(+)-K(+)-ATPase. *Am J Physiol* 1997; **273**: F857–F868.
58. Weiner ID, Verlander JW. Role of NH3 and NH4+ transporters in renal acid-base transport. *Am J Physiol Renal Physiol* 2011; **300**: F11–F23.
59. Livak KJ, Schmittgen TD. Analysis of relative gene expression data using real-time quantitative PCR and the 2(-Delta Delta C (T)) Method. *Methods* 2001; **25**: 402–408.
60. Carrisoza-Gaytán R, Salvador C, Bobadilla N *et al.* Expression and immunolocalization of ERG1 potassium channels in the rat kidney. *Histochem Cell Biol* 2010; **133**: 189–199.
61. Salvador C, Martínez M, Mora I *et al.* Functional properties of a truncated recombinant GIRK5 potassium channel. *Biochim Biophys Acta* 2001; **1512**: 135–147.
62. Constantinescu A, Silver R, Satlin LM. H-K-ATPase activity in PNA-binding intercalated cells of newborn rabbit cortical collecting duct. *Am J Physiol* 1997; **272**: F167–F177.
63. Liu W, Wei Y, Sun P *et al.* Mechanoregulation of BK channel activity in the mammalian cortical collecting duct (CCD): role of protein kinases A and C. *Am J Physiol Renal Physiol* 2009; **297**: F904–F915.
64. Roos A, Boron WF. Intracellular pH. *Physiol Rev* 1981; **61**: 296–434.
65. Heitzmann D, Warth R, Bleich M *et al.* Regulation of the Na+2Cl-K+ cotransporter in isolated rat colon crypts. *Pflugers Arch* 2000; **439**: 378–384.
66. Boyarsky G, Hanssen C, Clyne LA. Superiority of *in vitro* over *in vivo* calibrations of BCECF in vascular smooth muscle cells. *FASEB J* 1996; **10**: 1205–1212.